

We are IntechOpen, the world's leading publisher of Open Access books Built by scientists, for scientists

4,800

Open access books available

122,000

International authors and editors

135M

Downloads

Our authors are among the

154

Countries delivered to

TOP 1%

most cited scientists

12.2%

Contributors from top 500 universities



WEB OF SCIENCE™

Selection of our books indexed in the Book Citation Index
in Web of Science™ Core Collection (BKCI)

Interested in publishing with us?
Contact book.department@intechopen.com

Numbers displayed above are based on latest data collected.
For more information visit www.intechopen.com



The Emerging of Hydrovoltaic Materials as a Future Technology: A Case Study for China

Jiale Xie, Liuliu Wang, Xiaoying Chen, Pingping Yang, Fengkai Wu and Yuelong Huang

Abstract

Water contains tremendous energy in various forms, but very little of this energy has yet been harvested. Nanostructured materials can generate electricity by water-nanomaterial interaction, a phenomenon referred to as hydrovoltaic effect, which potentially extends the technical capability of water energy harvesting. In this chapter, starting by describing the fundamental principle of hydrovoltaic effect, including water-carbon interactions and fundamental mechanisms of harvesting water energy with nanostructured materials, experimental advances in generating electricity from water flows, waves, natural evaporation, and moisture are then reviewed. We further discuss potential applications of hydrovoltaic technologies, analyze main challenges in improving the energy conversion efficiency and scaling up the output power, and suggest prospects for developments of the emerging technology, especially in China.

Keywords: hydrovoltaic effect, carbon nanomaterial, electrokinetic effect, hydrovoltaic device, potential applications

1. Introduction

Water covers over 70% of the Earth's surface, which means it is abundant and widely available. Water contains enormous energy (35% of the solar energy received by the Earth, 10^{15} W) in a variety of forms, such as chemical, thermal, and kinetic energy [1]. The chemical energy is harnessed through water splitting under the assistance of electricity or photocatalysts [2]. The thermal energy is exploited for salinity power generation [3]. Kinetic energy is widely utilized by hydroelectric station, which is a main form of electricity.

As the progress of nanomaterials and nanotechnology, a new strategy based on hydrovoltaic effect (HV) has been developed in recent years [1]. In solar cells, the electron-hole pairs are generated by the absorption of photons with higher energy than the bandgap of semiconductor [4]. With the help of the built-in field at the interface of p-n junction, the electron-hole pairs are separated and then accumulated at the terminal of solar cells, generating photovoltaic voltage (**Figure 1a**). HV effect is analogous to the photovoltaic effect described as above. For HV effect, the potential is generated through the interaction between nanostructured materials and water molecules [1]. The form of water can be liquid, droplet, moisture, and

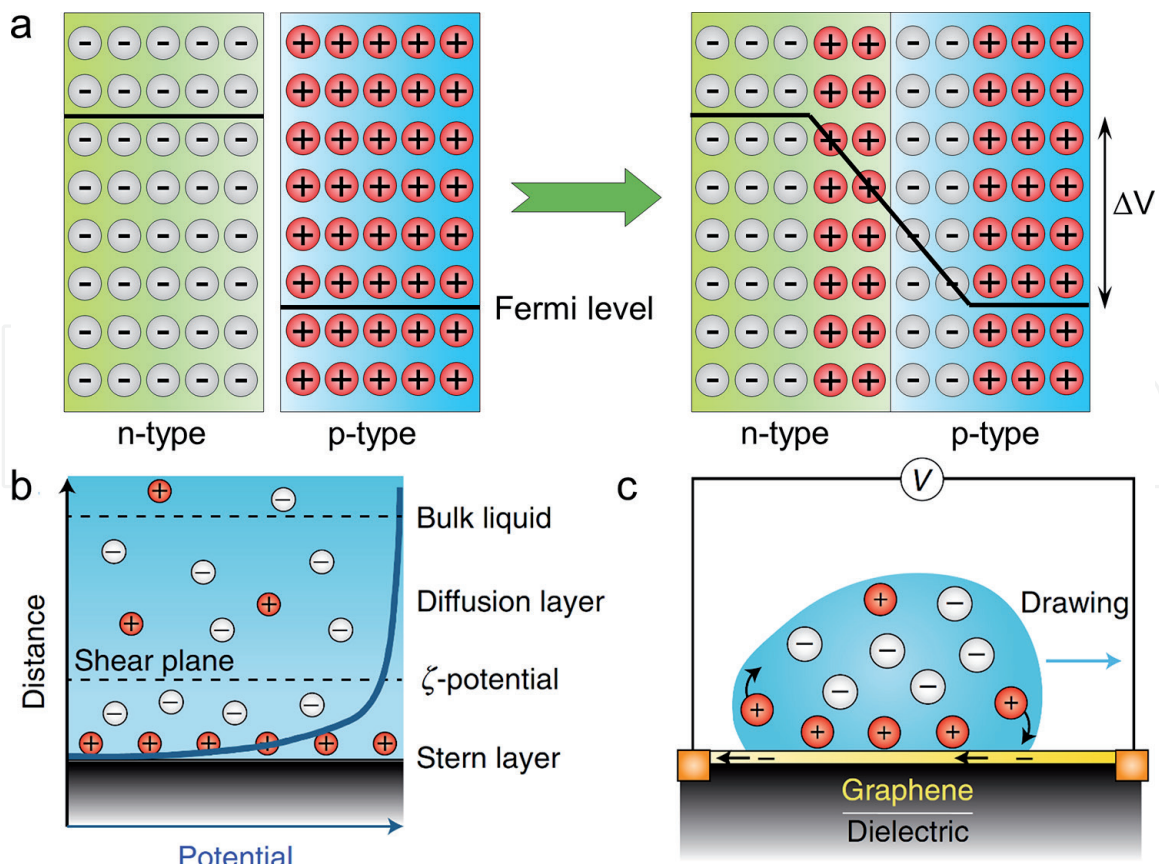


Figure 1.

(a) Photovoltaic effect with p-n junction. The basis of photovoltaic effect is the asymmetry of structural electronics. (b) Schematic of EDL forms at the solid surface with negative charges (not shown). There are two charge layers near the surface of solid, which are stern and diffusion layers. The stern layer is formed due to the chemical interaction between solid and absorbed ions. The diffusion layer electrically screen the stern layer through coulomb interaction. The blue line is the electrical potential curve around the solid surface [1]. (c) Illustration of induced potential by drawing a droplet on graphene. An electric current is formed in graphene by two moving boundaries of the EDL at the front and rear of the running droplet, respectively [1].

evaporation [5]. In brief, the basis of photovoltaic effect is the asymmetry of structural electronics (e.g., p-n junction). The nonuniformity of charge distribution at solid-liquid interface is the origin of HV effect. **Figure 1b** shows the electric double layer (EDL) at solid-liquid interface and the potential gradient as the distance increasing from solid surface into solution. **Figure 1c** illustrates the hydrovoltaic current is created in the graphene layer with the opposite orientation of the droplet flowing direction.

Since the HV phenomenon was discovered with carbon nanotubes (CNTs) in 2003, carbon nanomaterials were extensively investigated and considered as the most promising candidates for HV generators [6]. So far plenty of carbon nanomaterials exhibit HV effect with no need of a pressure gradient, including 0D graphene quantum dots (GQDs), 1D CNTs, 2D graphene or graphene oxide (GO), 3D graphene foam, and so on [7, 8]. Yet, unlike photovoltaic effect, research on the HV effect is in its infancy and calls for continued efforts to materialize its great potential. In this chapter, starting by describing fundamental principle of hydrovoltaic effect, including water-carbon interactions and basic mechanisms of harvesting water energy with nanostructured materials, experimental advances in generating electricity from water flows, waves, natural evaporation, and moisture are then reviewed. We further discuss potential device applications of hydrovoltaic technologies, analyze main challenges in improving the energy conversion efficiency and scaling up the output power, and suggest prospects for developments of the emerging technology.

2. Fundamentals of hydrovoltaic effect

2.1 Mechanisms of hydrovoltaic effect

2.1.1 Electric double layer and pseudocapacitance mechanism

As in **Figure 2a**, in a nanochannel, the EDL layers form on the interface of solid–liquid and overlap each other due to the small size of nanochannel. Under pressure gradient, a steady current will be generated along with the ion transport from high to low pressure side. The voltage will prohibit the transport of more ions. Therefore the steady current named the streaming current is generated [9]. There is positive correlation between the flow rate, pressure gradient, channel height, and the streaming current.

When a nanomaterial (e.g., graphene) is inserted into the liquid level, the EDL layer will be created and changed as the immersed area of nanomaterials changes. This means, if the immersed area increases, the EDL layer will be charged and a voltage will be generated in the nanomaterials (**Figure 2b**). On the contrary, an inverse voltage can be observed due to the discharging of EDL layer. This wave-induced voltage was called waving potential [10]. The voltage and current are proportional to the velocity of graphene and can be scaled up by series and parallel connections of multiple graphene devices.

When the water contained ions is a droplet on graphene, the EDL is emerged only in the region of droplet followed the EDL theory. When the droplet is moving under the external force such as gravity, the EDL region will move accordingly. During this moving process, there is a charging state at the front of the droplet, while a discharging process at the rear of the droplet (**Figure 1c**). Therefore an electrical voltage called as drawing potential can be generated [11]. The voltage and current will increase as the velocity and number of droplets increase. The drawing potential can be developed to harvest raindrop energy (**Figure 2c**).

2.1.2 Ion diffusion-induced mechanism

When moisture were adsorbed by nanomaterials with oxygen-containing functional groups, a gradient of H^+ can form because of the local solvation effects, which can lead to the breakage of $O^{\delta-}-H^{\delta+}$ bonds. Due to the H^+ concentration difference, the H^+ will migrate along the reverse gradient direction. Then a voltage would increase continuously until the gradient of H^+ vanishes. When the ingress of moisture stopped, the number of migratory ions decreased as free H^+ and oxygen-containing functional groups recombined, resulting in an reverse voltage [12].

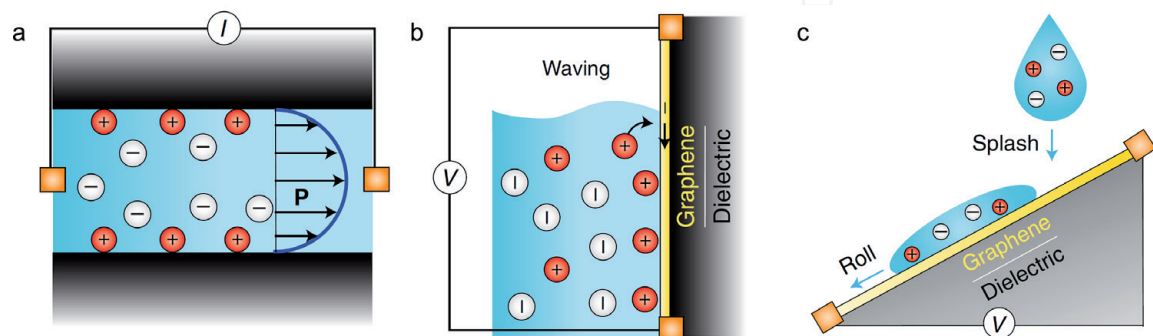


Figure 2. (a) Schematic of electrokinetic effect in the nanochannel. Blue line illustrates the profile of flow velocity through the nanochannel [1]. (b) Illustration of waving potential induced in graphene by one moving boundary of EDL across a graphene sheet on a dielectric substrate [1]. (c) Schematic illustration of harvesting energy from raindrops [1].

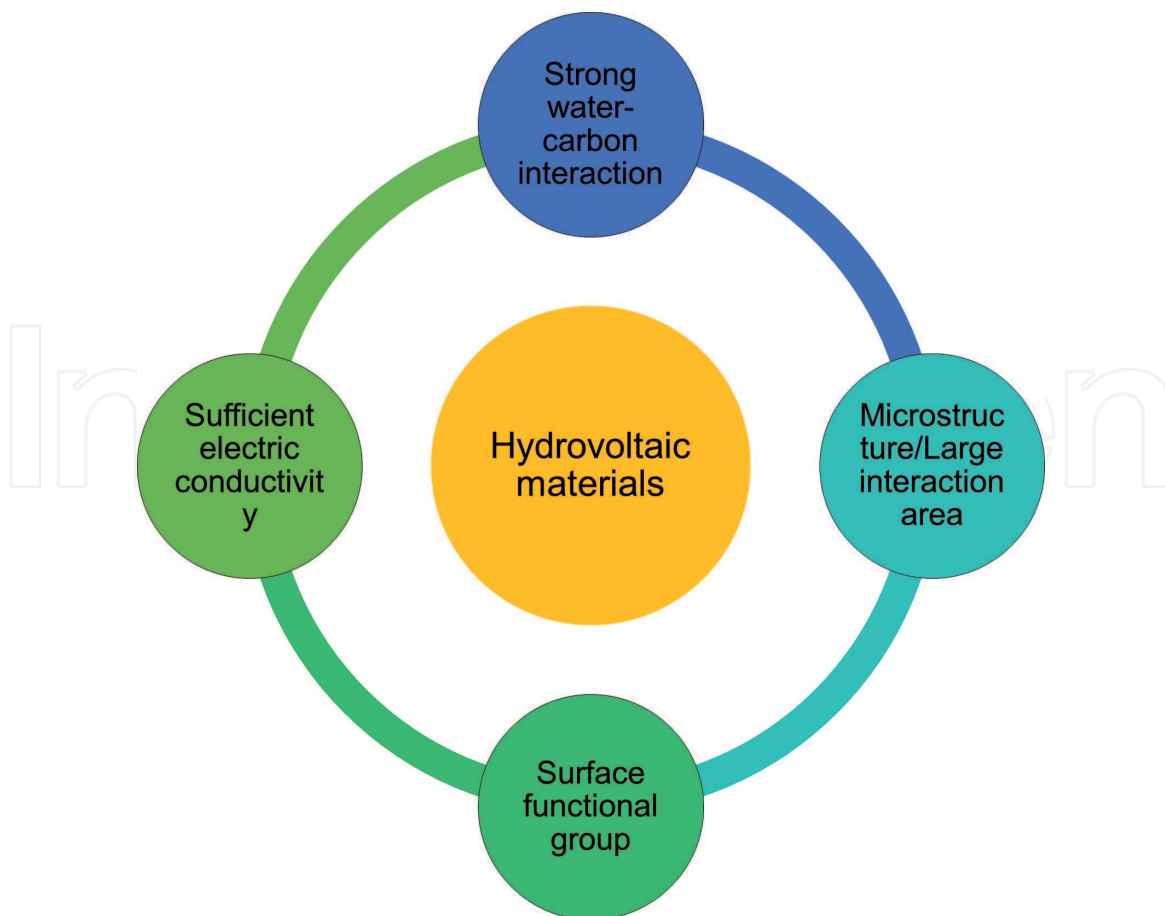


Figure 3.
Characteristics of a good hydrovoltaic material.

2.2 Rules for hydrovoltaic material

Based on the above discussion of mechanisms, an excellent hydrovoltaic material should possess the following characteristics: strong water-carbon interaction, rational pore and microstructure for the transport of water molecules, large interaction area for water adsorption and charge storage, sufficient electric conductivity for charge transportation, and abundant/gradient surface functional groups (oxygen functional groups in particular). Nowadays, the most reported hydrovoltaic materials are carbon nanomaterials [7, 8]. However, the hydrovoltaic effect is not limited to carbon nanomaterials but can be generic to other materials as long as they meet the above characteristics (**Figure 3**).

3. Hydrovoltaic devices and performance

3.1 Moisture-induced electricity generation

Moisture is one important form of water in the nature. GQDs have unique properties due to quantum confinements and edge effects [13]. GQDs as the chemically active material have fabricated a moisture-triggered generator [14]. The size of GQDs is 2–5 nm. The GQDs contain an amount of oxygen-containing functional groups. To create a gradient of functional groups, GQDs are treated via electrochemical polarization. The GQD generator achieves a high voltage of 0.27 V, when the variation of relative humidity (RH) is 70%. After the optimization of the

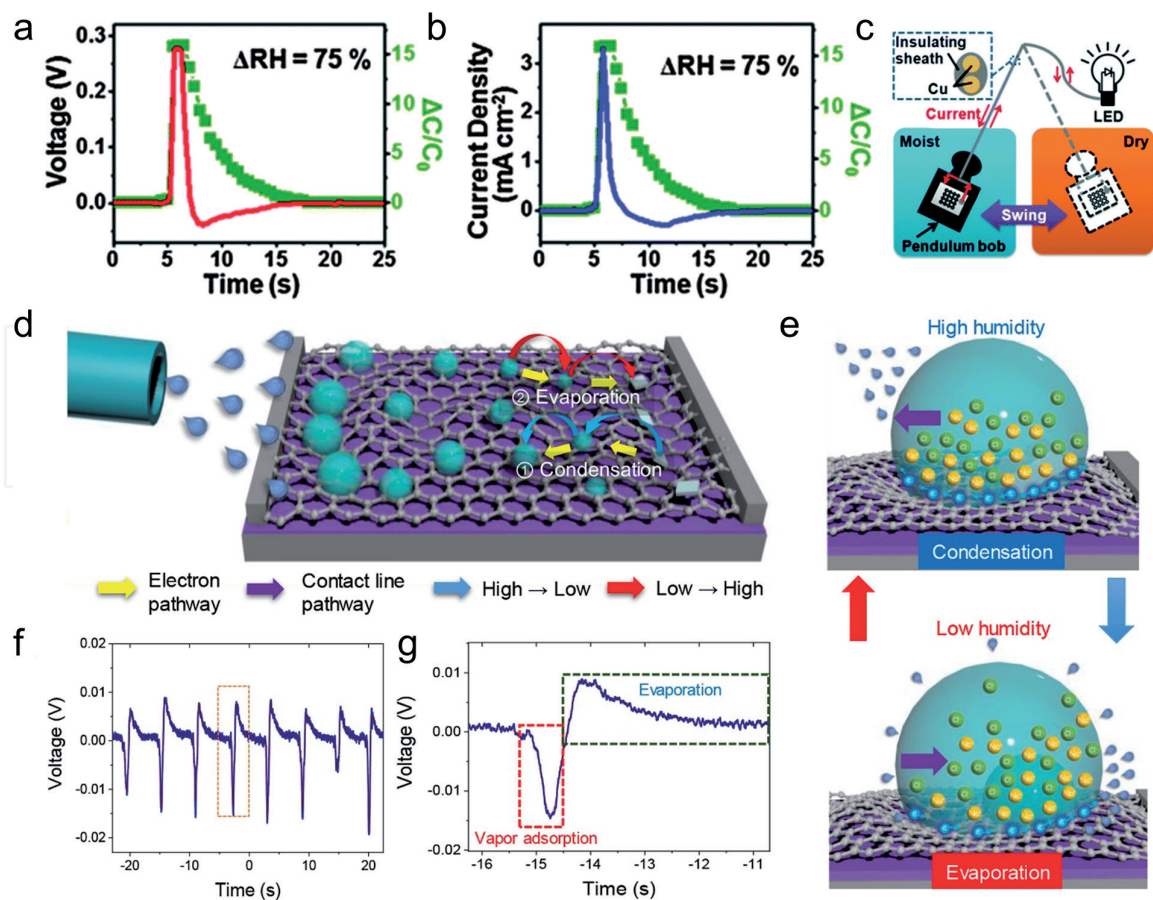


Figure 4. (a) Voltage and (b) current output cycle of HV device based on g-3D-GO that is sandwiched by aluminum electrodes in response to the RH variation ($\Delta RH = 75\%$) [16]. (c) Schematic illustration of a HV device-based power source system [16]. (d) Schematic illustration of the mechanism of humidity-driven electricity generation. [17] (e) Condensation and evaporation of ionic liquids under different humidity [17]. (f and g) Voltage generated with wrinkle graphene/salt crystal nanogenerator under a sudden change in humidity [17].

load resistor, a power density obtained is 1.86 mW/cm^2 . The gradient of oxygen-containing functional groups is the reason of electricity generation with moisture. Similarly, the porous carbon black, and GO framework with the functional group gradient, can also exhibit excellent HV performance under moisture [15, 16]. For example, a superhydrophilic 3D assembly of graphene oxide (g-3D-GO) with open framework exhibits a high power density of ca. 1 mW/cm^2 and an energy conversion efficiency of ca. 52% [16]. With an RH variation of 75%, the g-3D-GO-based HV device could provide a voltage and current output of ca. 0.26 V and ca. 3.2 mA/cm^2 within 2 s (**Figure 4a** and **b**). As in **Figure 4c**, a power source system consists of four HV cells in series which was fabricated to demonstrate the practical application. This system was attached onto the pendulum bob. The pendulum bob can swing between moist region (RH = 80%) and dry region (RH = 5%). When the system moves to the moist region, the moisture-induced positive voltage is applied on the light emitting diode (LED), and it lights up. Upon traveling to the dry region, the LED will switch off. As a consequence, this power source system could provide a steady power output.

Recently, Zhen et al. prepared a nanogenerator using the wrinkled graphene, which followed an unusual mechanism of HV effect [17]. In this work, a new cation- π interaction utilization strategy was developed. In other words, electricity is generated through water adsorption and desorption of salt crystals along with the humidity variation. The key of this nanogenerator is to deposit salt crystals onto the wrinkled graphene by manipulating the formation of ionic liquid microdroplets.

The wrinkled graphene has many defects and uniform wrinkles, facilitating the ultrafast water evaporation, preventing excessive water accumulation and deposition of well-distributed salt crystals. **Figure 4d** and **e** schematically illustrates the mechanism of electricity generation. As the sudden change of humidity (25–75–25%), two inversed voltage peaks were observed sequentially (**Figure 4f**). This is attributed to the water vapor adsorption and desorption on the salt crystals. The sharper negative peak is due to the strong water adsorption ability of the salt crystals, while the broad positive peak is from the slow desorption process (**Figure 4g**). The voltage of 18 mV with the current of 37 nA was achieved with a $1 \times 6 \text{ cm}^2$ generator. Among various salts, NaCl exhibits the best performance due to its complete crystallization after each cycle.

As far as we know, the nanomaterials for moisture-induced electricity generation include carbon/graphene quantum dots, carbon black, GO film, and 3D GO frameworks. The main origin of electricity generation is similar to each other. The potential generation is dependent on the water adsorption difference due to the gradient of oxygen-containing functional groups and induced the concentration difference of charge carriers. Interestingly, the porous carbon black film treated partially by plasma could generate continuous electricity, which is totally different from other carbon nanomaterials. This discrepancy may be from the difference of the structure and/or the introducing manner of functional groups.

3.2 Electricity generation induced by droplet movement

In 2014, Yin et al. firstly reported the electricity generation induced by droplet movement on monolayer graphene [11]. When a droplet of 0.6 M NaCl is drawn on graphene at a constant velocity of 2.25 cm/s, a voltage of 0.15 mV is generated. When the direction of droplet movement is opposite, the direction of potential is also reversed. When the movement is stopped, no potential is produced. Rain is one of important existent forms of water in nature. However, the energy in the rain is not yet utilized efficiently in the long term. There are amount of cations (such as Na^+ , NH_4^+ , Ca^{2+} , Mg^{2+}) and anions (such as Cl^- , NO_3^- , SO_4^{2-}). Therefore harvesting energy from rain using HV effects is a promising approach [18, 19].

As previously reported, the low generated voltage of around 0.15 mV, and the external pressure needed, would limit the application of HV effect. Recently, Li et al. reported the electricity generation from water droplets on porous carbon film through capillary infiltrating [20]. **Figure 5a** illustrates the structure of the porous carbon film (PCF) device. When a droplet of 1 μL was dropped onto PCF, a sustainable voltage of 0.3 V was generated (**Figure 5b**). However, electricity generation by droplet movement on graphene or aligned single-walled nanotubes is pulse-like. The retention of voltage depends on the volume of water droplets as shown in **Figure 5c**, but the generated voltage value is nearly identical. More interesting, the dropping position of water droplet would influence the induced voltage (**Figure 5d**). Experimental results reveal the following key characteristics: (i) the merely directional water infiltration can induce the voltage, (ii) no direct correlation between the HV voltage and the position of droplets, and (iii) the direction of water infiltration influences the voltage sign. At last, the authors demonstrated a scale-up application with three devices in series (**Figure 5e**). Twelve 5 μL water droplets can generate a voltage up to 5.2 V and illuminate a liquid crystal display. This work powerfully demonstrate that a hydrophilic porous carbon film with water droplets could realize the energy harvested from rain and a practical application. However, there is no experimental results in real raining environment. More information on the droplet-induced electricity generation can refer one recent review paper [21].

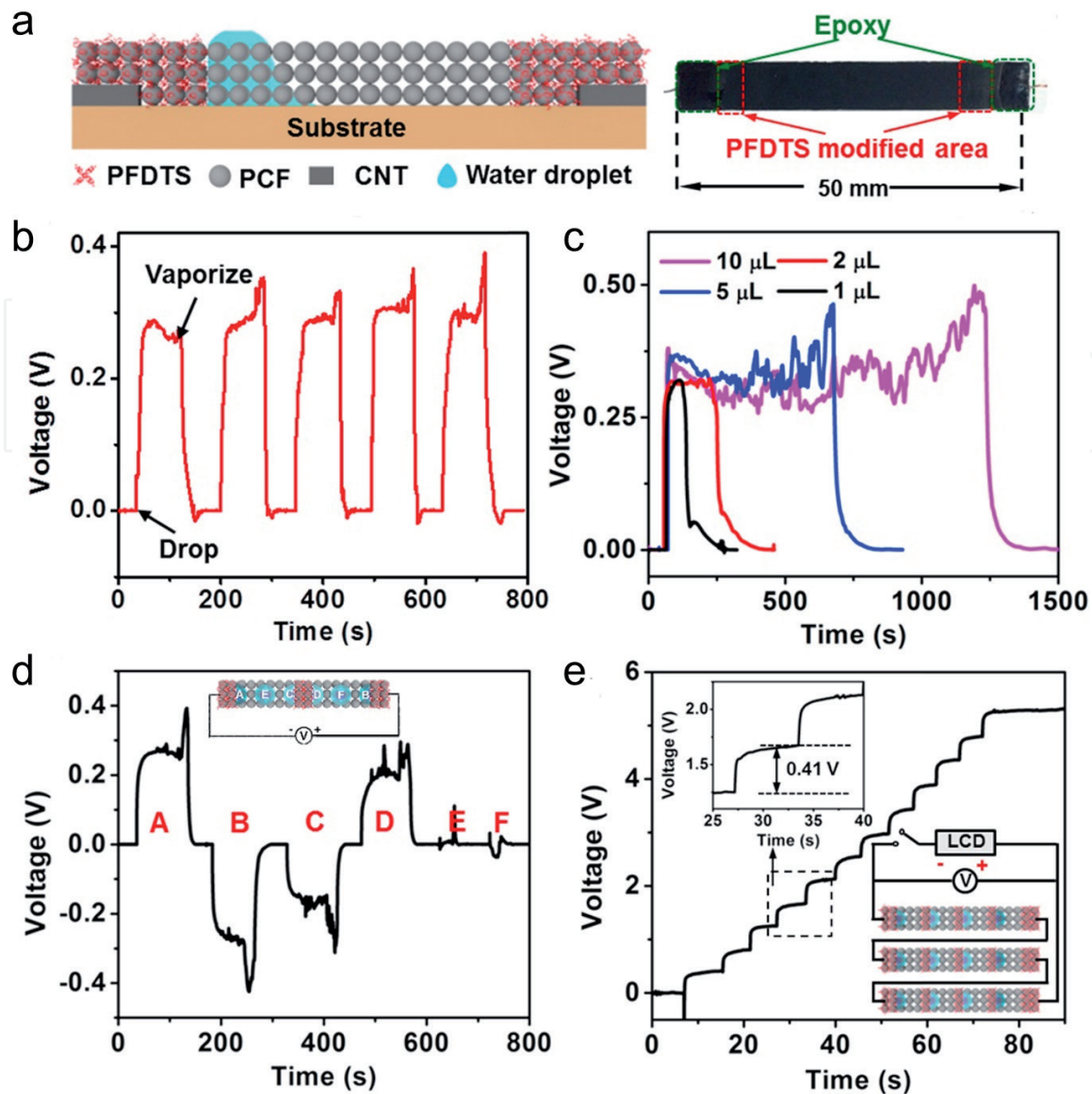


Figure 5.
 (a) Schematic of the porous carbon film device with two ends modified with 1H,1H,2H,2H-perfluorodecyltriethoxysilane (PFDTs). The right inset shows a photograph of a typical device with dimensions of $50 \times 7 \text{ mm}^2$ [20]. (b) Open-circuit voltage obtained by repeatedly dropping $1 \mu\text{L}$ water droplets at the PFDTs@PCF/PCF interface under ambient conditions ($\sim 23.5^\circ\text{C}$ and $\text{RH} \sim 71.7\%$) [20]. (c) Measured V_{oc} vs. time of the device when water droplets with various volumes were dropped onto the PFDTs@PCF/PCF interface [20]. (d) Wetting dependence of the induced voltage. Inset is schematic of the V_{oc} measurement and the water-droplet position [20]. (e) Application demonstration of the water-droplet-induced voltage [20].

3.3 Flow-induced electricity generation

Ocean wave energy is a main form of ocean energy, which is considered as inexhaustible energy. In 2007, Liu and Dai reported that the flow-induced voltage can be greatly improved by aligning the nanotubes along the flow direction [23]. In 2017, Xu et al. fabricated a fluidic nanogenerator fiber with the aligned multi-walled carbon nanotube sheet (inset of **Figure 6b**) [22]. The device shows a power conversion efficiency of 23.3% and an excellent stability over 1,000,000 cycles. The flow direction, the flow distance, the flow velocity, and the NaCl concentration are positive correlation with the induced voltage (**Figure 6a–6c**). The authors also discovered that the ordered mesoporous carbon (OMC) can significantly enhance the flow-induced voltage (**Figure 6d**). After OMC introduction, the sustained voltage for over 1 h can be achieved. The maximum voltage output can reach up to 341 mV when the content of OMC is $5.1 \mu\text{g}/\text{cm}$. Impressively, the stable performance of this

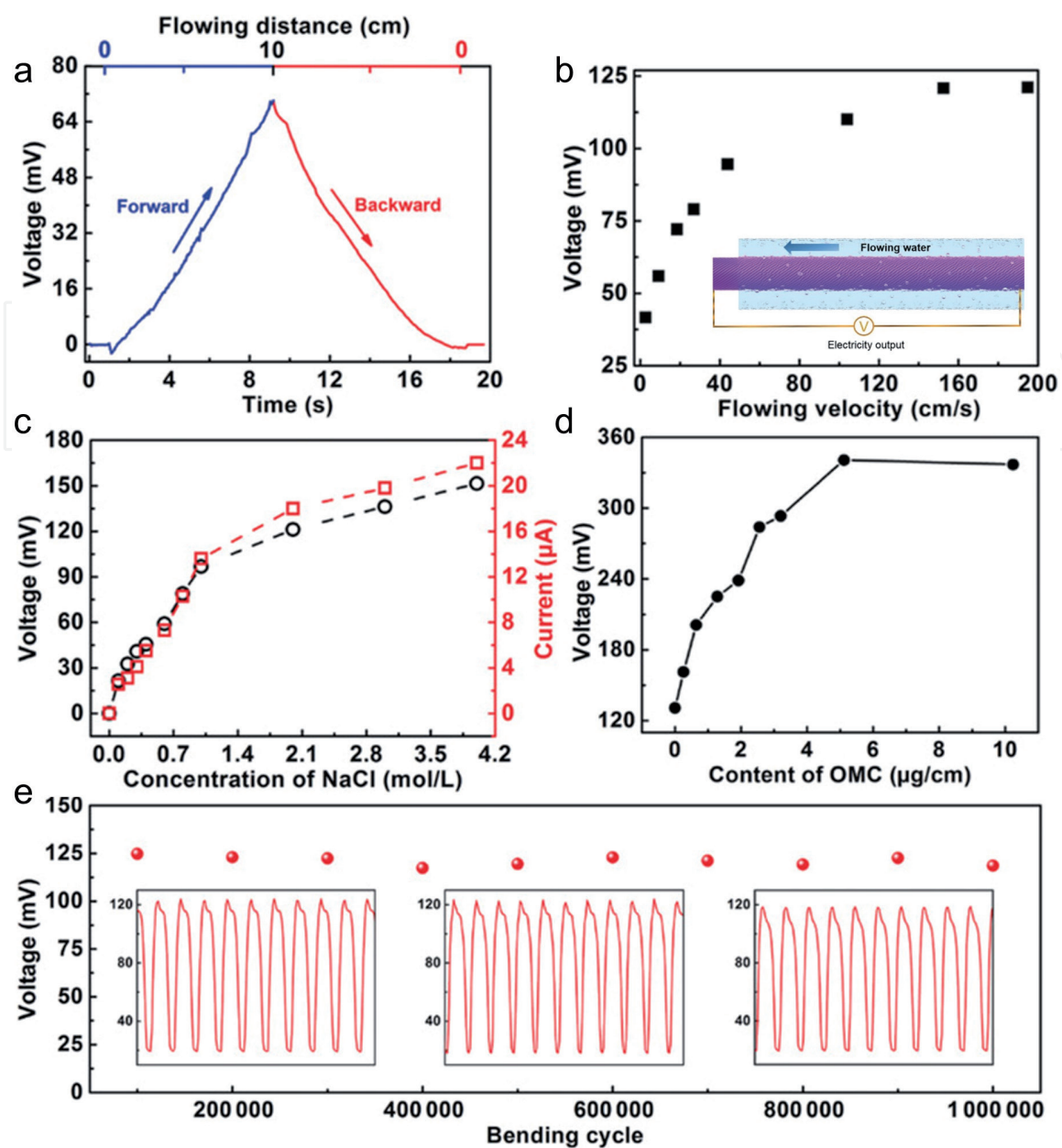


Figure 6. (a) Voltage curve induced by a saturated NaCl flow at the velocity of 1.2 cm/s [22]. (b) Relationship between the voltage and the flow velocity. Solution is 0.6M NaCl [22]. (c) The voltage vs. current relationship as the concentration variation of NaCl solution (flow velocity: 12.9 cm/s) [22]. (d) Dependence of the voltage on the OMC content in a saturated NaCl solution (flowing velocity: 20 cm/s) [22]. (e) Voltage generated by repeatedly dipping an OMC-incorporated device into a NaCl solution with an increasing number of bending cycles. The inserted graphs show the voltages after 200,000; 600,000; and 1,000,000 bending cycles in the NaCl solution [22].

device can be maintained even after over 1,000,000 bending cycles (**Figure 6e**). Moreover, the fiber nanogenerator is flexible and stretchable, indicating it can be woven into fabrics for large-scale applications.

Two-dimensional materials or devices have more advantages for ocean wave energy harvesting, which can well float on the surface of the ocean [1, 25]. Recently, Fei et al. achieved volt leveled waving potential using a pair of graphene sheets [24]. **Figure 7a** illustrates the device setup, where a pair of graphene-PET sheets with size of $2.5 \times 1.5 \text{ cm}^2$ is immersed in NaCl solution. As one of the graphene sheets moves through the liquid surface, electricity is generated (**Figure 7b**). The peak voltage can be around 60–120 mV. However, no voltage is observed either moving graphene underneath or parallel to the liquid level, indicating the waving potential is due to the dynamic EDL boundary. In this setup, the moving graphene is served as driving force for ion movement, while another graphene is as a reference electrode.

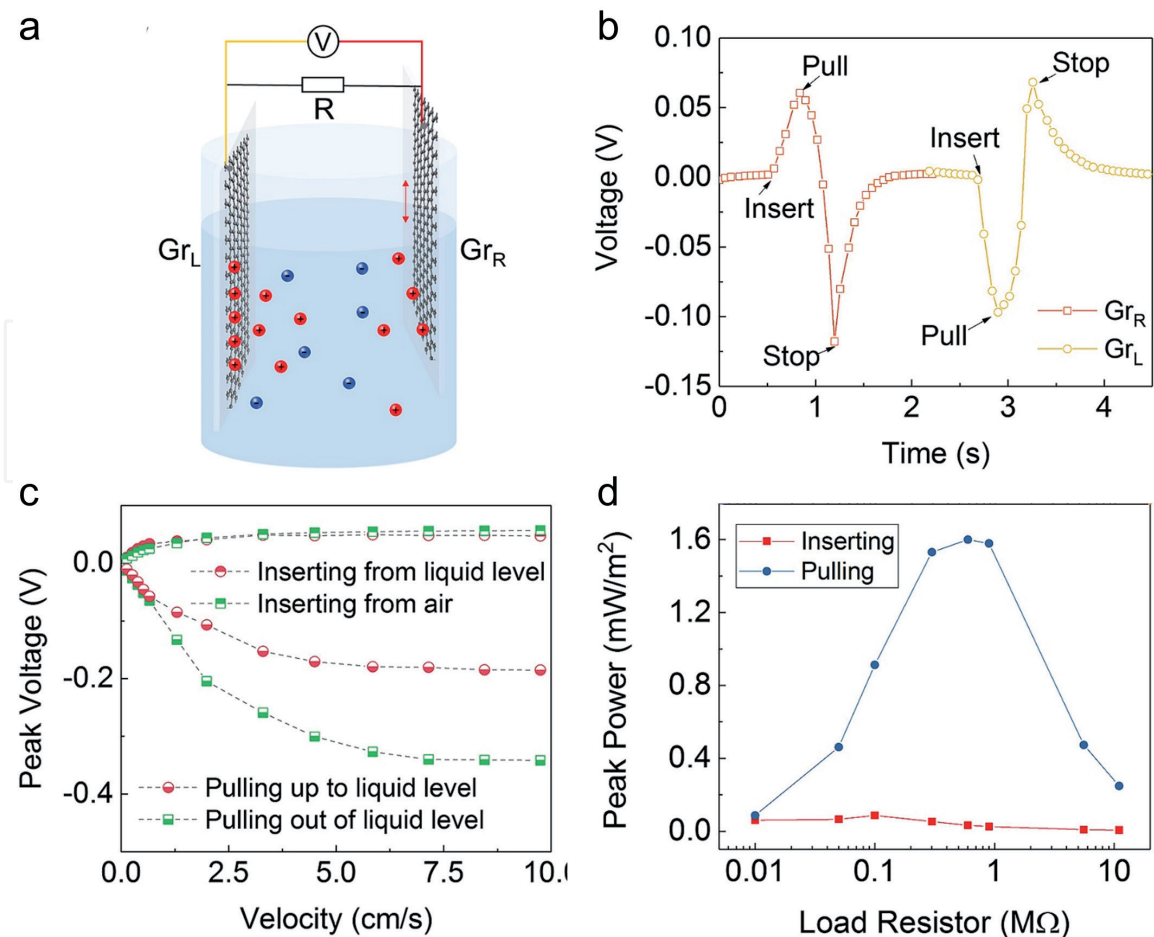


Figure 7. (a) Schematic of experimental setup with two graphene-PET sheets immersed vertically in an electrolyte container. Gr_L and Gr_R represent graphene samples on the left and right side, respectively [24]. (b) Generated voltage signals at resistor of $0.9\text{ M}\Omega$ when separately moving Gr_L or Gr_R across NaCl solution [24]. (c) Peak voltage values collected as a function of velocity. The perpendicular moving distance of graphene is kept as 2 cm [24]. (d) Calculated output power per unit area of graphene [24].

Figure 7c shows the relationship between the peak voltage and the moving velocity of graphene. The peak voltage exhibits linear relations with velocity at low moving speeds and saturates to certain values at high speeds. This saturation may be due to the limit from the speed of ion adsorption/desorption. During the pulling process, when the load resistance is $0.6\text{ M}\Omega$, the largest power density of 1.6 mW/m^2 can be obtained (**Figure 7d**). Moreover, the ion species can also influence the voltage value. The peak voltage values follow an order of $\text{LiCl} > \text{NaCl} > \text{KCl} > \text{BaCl}_2$, indicating the smaller ions are better for higher voltage generation.

Apart from the dynamic EDL boundary mechanism, the water-carbon interaction can also generate electricity [26]. In this case, the water does not need the cations and anions for the formation of EDL capacitance. More importantly, the electric signals are continuous, but the inherent mechanism is not very clear yet. More information on the liquid flow-induced electricity in carbon nanomaterials can refer the recent review papers [27, 28].

3.4 Evaporation-induced electricity generation

Water evaporation is a crucial step in the natural water circulation, releasing a huge amount of water energy. In 2017, Xue et al. reported that the water evaporation from centimeter-sized carbon black sheets can reliably generate sustained voltages of up to 1 V for 8 days under ambient conditions [29]. The annealing and plasma treatment introduced functional groups are essential for the electricity generation.

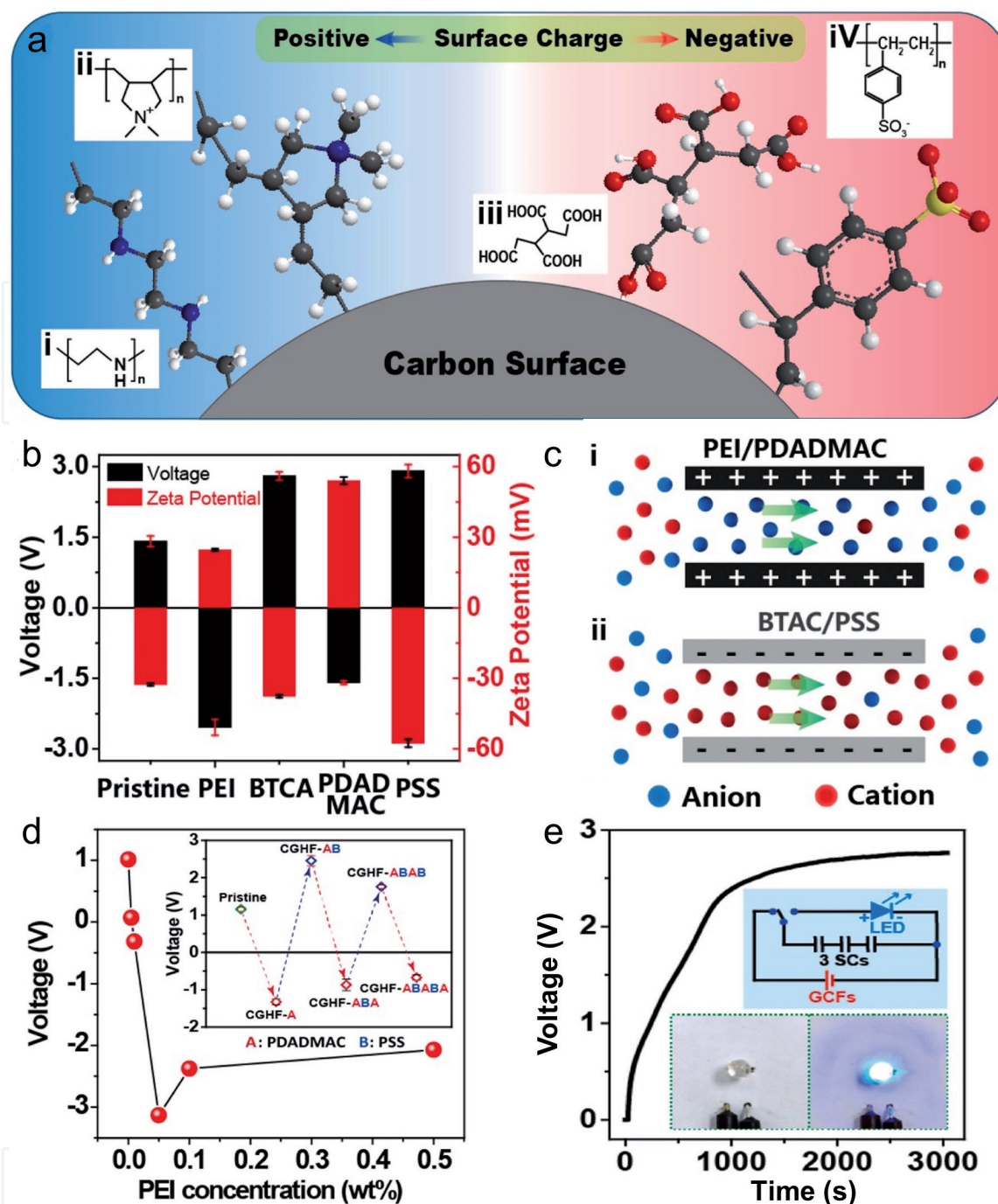


Figure 8. (a) Schematic of the chemical modification with different molecules on carbon nanoparticles [30]. (b) V_{oc} and zeta potentials of the pristine and modified GCFs [30]. (c) Schematic of the ion-selective transport mechanism in the nanochannels with (i) positively and (ii) negatively charged surface [30]. (d) Dependence of V_{oc} of the device on the PEI concentration. The inset shows the evolution of V_{oc} when a GCF was repeatedly modified by DADMAC(A) and PSS(B) [30]. (e) Voltage-time curve of three supercapacitors (SCs) connected in series in charging by the GCFs at ambient condition. Insets show the circuit diagram (top) and photos of the blue LED. [30].

Recently, Li et al. fabricated an evaporation-driven nanogenerator ($1\text{ cm} \times 5\text{ cm}$) with a high open-circuit voltage of 3 V [30]. The film device is fabricated using carbon black and glass fiber. As in **Figure 8a**, the surface of the hybrid film was modified with several polymer molecules, such as polyethylene imine (PEI); 1,2,3,4-butane tetracarboxylic acid (BTCA); polydimethyl diallyl ammonium chloride (PDADMAC); and poly sodium-p-styrenesulfonate (PSS). The voltage of the glass-fiber-carbon-nanoparticle film (GCF) can vary from -3 V to 3 V , which rely on the difference of the surface functional groups (surface charges) as in **Figure 8b**. PEI- and PDADMAC-modified GCF have positive surface charges and thus positive

zeta potentials. The ion-selective transport mechanism is schematically shown in **Figure 8c**. The concentration of polymer solution is one of critically experimental conditions, which can significantly affect the voltage from +1 V to −3.2 V by using 0–0.5 wt% PEI solution (**Figure 8d**). There is an optimal concentration of PEI solution (0.05 wt%), which should be attributed to the low conductivity of polymer and/or the partial channel blocking. A hybrid film device using two GCFs with opposite surface charges was also prepared. Therefore the generated voltage was enhanced to around 5 V (5 × 5 cm). They also connected the hybrid film device with supercapacitor. The supercapacitor can store the electric energy from GCFs and provide a high current output. The supercapacitor can be charged up to 2.8 V by the output voltage of GCFs, and then a blue LED can be lighted up for about 10 s without any auxiliary. This work shows the great potential of evaporation-induced electricity generation in the field of portable electronics.

4. Potential applications

4.1 Self-powered liquid sensors

Because of the low power density (10^{-3} – 10 W/m²) of HV device, [1] it is a good choice to develop HV effect-based self-powered devices, such as self-powered liquid sensors. The factors which can affect the HV signal could be used for sensing applications, including flow rate, fluid volume, solution component, fluid movement, and so on. Yin et al. developed a monolayer graphene-based HV device in 2013 and demonstrated the self-powered liquid sensor application [11]. The configuration of HV devices is shown in **Figure 9a**. A droplet of 0.6 M NaCl was moved with a SiO₂/Si wafer on the graphene film. During the moving of the droplet, the advancing and receding contact angles are ~91.9° and ~60.2°, respectively. As in **Figure 9b**, the

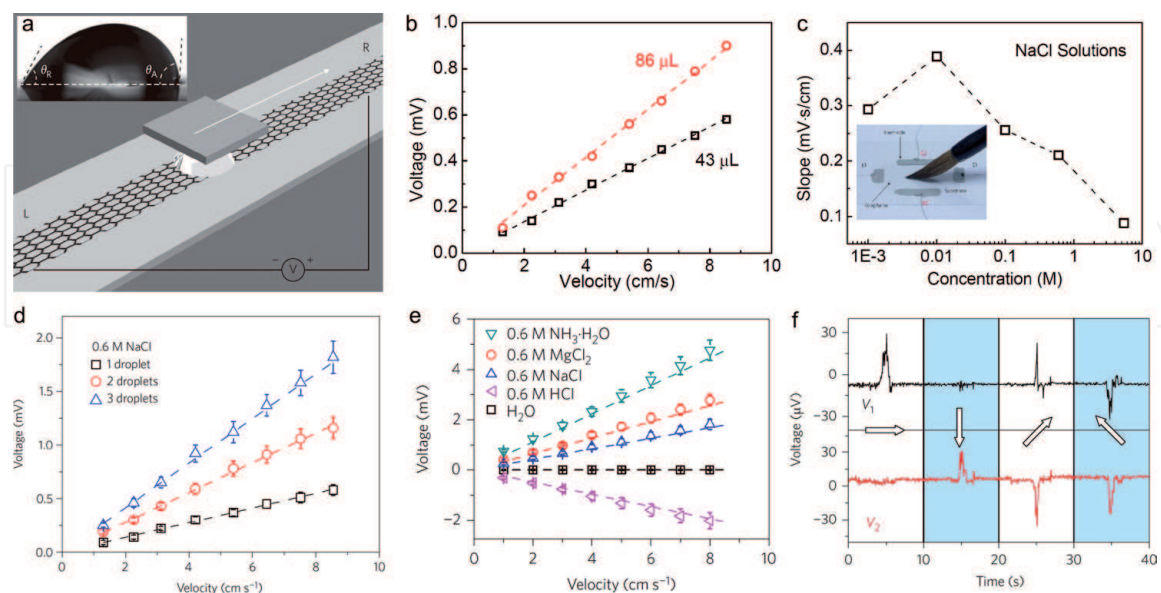


Figure 9.

(a) A liquid droplet is sandwiched between graphene and a SiO₂/Si wafer and drawn by the wafer at specific velocities. Inset: A droplet of 0.6 M NaCl on a graphene surface [11]. (b) Dependence of the output voltage on the volume of a droplet of 0.6 M NaCl [11]. (c) Dependence of the output voltage on the concentration of the solution (three droplets of NaCl solution). Inset: Photograph of handwriting with a Chinese brush on graphene [11]. (d) Voltage induced by moving one, two, and three droplets of 0.6 M NaCl. Dashed lines are curves linearly fitted to the measured data [11]. (e) Voltage for various ionic solutions (three droplets) on monolayer graphene [11]. (f) Sensing the stroke directions (arrows) by the drawing potentials between electrodes E₁⁺–E₁[–] and E₂⁺–E₂[–] as shown in the inset of c [11].

voltage of device is linearly proportional to the velocity of droplet. The larger the size of the droplet would induce the larger voltage. The concentration of NaCl solution is also a critical factor, but the trend is not monotonic. The best concentration of NaCl solution is around 0.01 M. The voltage output is less than 0.5 mV. However, in carbon black, the potential is maximum ~ 1.0 V when deionized (DI) water is used for evaporation HV generator [29]. It is interesting that the voltage can be multiplied by drawing multiple droplets simultaneously as shown in **Figure 9c**. Experimental results indicate the voltage is near zero when two droplets are moving in the opposite directions. The voltage of device is closely related to the ion species, such as MgCl_2 , HCl, and $\text{NH}_3 \cdot \text{H}_2\text{O}$. However, there is no response for DI water. This indicates the drawing potential comes from the ion-induced EDL capacitance. The voltage induced with HCl solution is negative. The authors think that there is a H_3O^+ layer on the surface of graphene. Therefore the positively charged graphene would attract the negative Cl^- anions, which dominate the electric double layer. At last the authors show a handwriting sensor with a Chinese brush and 0.01 M NaCl. Two pairs of electrodes, $E_1^+ - E_1^-$ (right-left) and $E_2^+ - E_2^-$ (bottom-top), were patterned perpendicularly on the four sides of the graphene to distinguish the handwriting direction (inset of **Figure 9c**). The drawing direction related to voltage signal can be well detected as in **Figure 9f**. Moreover, the force and speed of the handwriting can also be monitored.

Graphene oxide framework with lots of pores can facilitate the diffusion of water molecules. Along with the asymmetrical oxygen-containing groups, Zhao et al. observed that the transport of the ionic charge carriers is accelerated due to the ionic gradient [16]. When the RH variation is 75%, the potential can increase up to 260 mV in 2 s. The concentration gradient of Li ions in 3D PPy framework can also show good sensitivity for moisture [31]. The potential is 60 mV under the RH variation of 85%. More importantly, the stability of this material is stable during the several hundred cycles.

Besides the HV potential, other signals can also be utilized for sensing, such as the resistance of materials, the length of fibers, and the volume of materials [32–36]. Of course, the change of other physical fields, such as temperature and wind speed, can be detected by HV devices directly or indirectly [29, 37].

4.2 All-weather power generation

As we all know, the common solar cells only work on sunny days, but do not work in the night and on rainy days. Combining PV and HV effects, a hybrid cell for all-weather power generation was developed by integrating a solar cell with a HV device. Tang et al. fabricated a flexible solar cell made of a transparent graphene electrode and a dye-sensitized solar cell [38]. The hybrid cell can be excited by solar light on sunny days and raindrops on rainy days, yielding a solar-to-electric conversion efficiency of 6.53% under AM 1.5 irradiation and power in the range of 5.12–54.19 pW by simulated raindrops (**Figure 10b**). However, the output of this hybrid cell is still far lower than the actual requirement. Then Tang et al. changed the graphene to graphene/carbon black/polytetrafluorethylene (PTFE) for the hybrid cell fabrication [18]. But the voltage and current did not show significant improvement under simulated raindrops. Zhong et al. developed a 2D hybrid nano-generator based on graphene and silicon for all-weather electricity generation [39]. In this hybrid cell, the graphene and silicon form the van der Waals Schottky diode (**Figure 10c**). This hybrid device delivers a maximum output power of 49.3 μW under light illumination. When the DI water flows on the graphene under light from Au electrode to Ag electrode, an additional potential of 2.54 mV can be generated (**Figure 10d**). However, there is no response in the dark, indicating no interaction

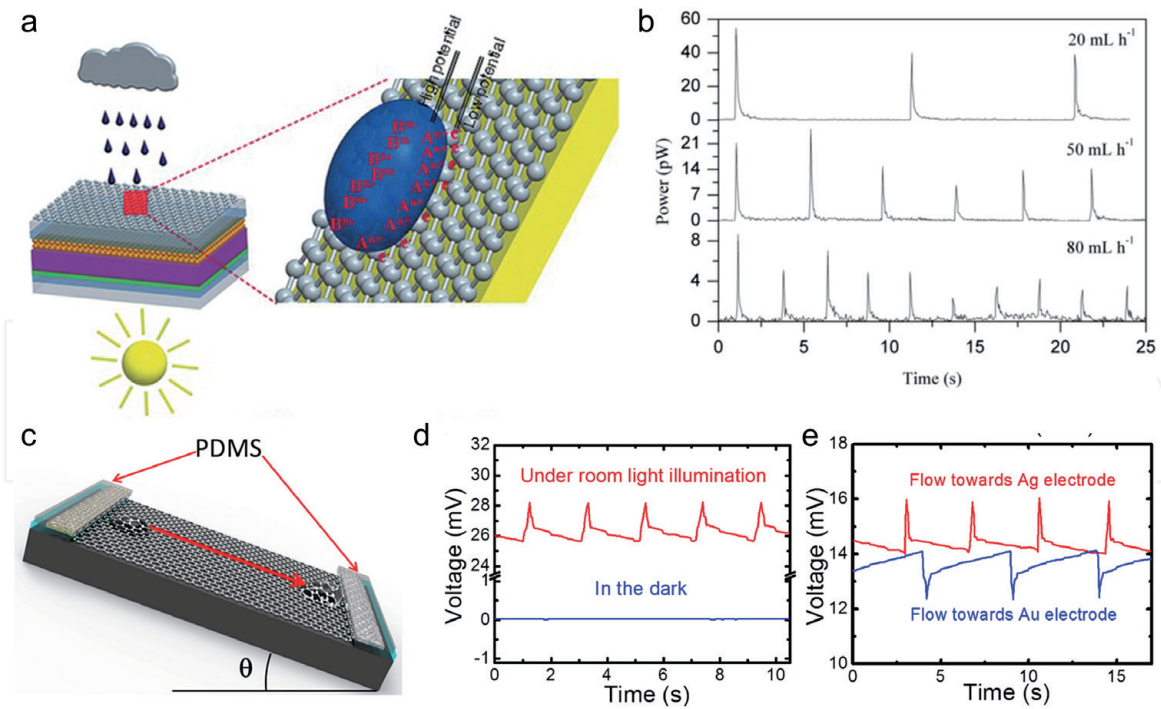


Figure 10. (a) The quasi-all-weather solar cell that can produce electricity from rain and sun [38]. (b) Power signals produced by dropping 0.6 M NaCl droplets on rGO film [38]. (c) Schematic structure of the 2D hybrid nanogenerator of graphene/SiO₂/Si [$\theta = 30^\circ$, PDMS: Poly(dimethylsiloxane)] [18]. (d) Voltage responses to the flow of DI water over graphene/Si Schottky diode in the dark and under room light illumination [18]. (e) Voltage responses to the flow of DI water toward different directions [18].

exists between water and hybrid cell during the water flowing process. The authors think that the potential response should arise from the interaction between water and graphene/Si Schottky diode (the doping and dedoping at the front and rear side of water droplet, respectively) instead of the water-graphene interaction or the water-electrode interaction. Moreover, the negatively additional potential can be observed when the water flows toward Au electrode. This phenomenon should be attributed to the asymmetric potential profile of the graphene channel.

4.3 Harvesting Ocean wave energy

Due to the intermittency and randomness of raining, it is wise to harvest energy from the ocean wave energy. The ocean wave energy is renewable and inexhaustible because 70% of the Earth's surface is covered by the ocean. The ocean wave energy is also called as blue energy [40]. Tan et al. fabricated a film type wave energy generator with graphene, carbon black, and polyurethane [25]. A voltage of > 20 mV and a current of > 10 μ A are produced in a 15 cm²-sized generator. Moreover, the devices are sustainably stable upon persistent attack by waving ocean. The floating devices on the sea can be packaged into the wave energy stations by series and parallel connections. Tan et al. further proposed a photo-induced charge boosting liquid-solid electrokinetic generator with a structure of polyurethane/graphene oxide-carbon black-multi-walled carbon nanotube/carbon quantum dots/copper (PU/GO-CB-MWCNT/CQDs/Cu) [41]. Under AM1.5 illumination, the voltage, current, and power density achieved by this device are 0.1 V, 0.39 mA, and 26.6 mW/m², respectively. The working mechanism is described in **Figure 11a-c**. Due to the difference of Na⁺ and Cl⁻ ions on adsorption energy, the EDL can be formed. Same as the principle of waving potential as above, the potential signal would change along with the seawater moving and the capacity change. **Figure 11d** presents an enlarged one-cycle electrical signal generation. When the seawater moves to the

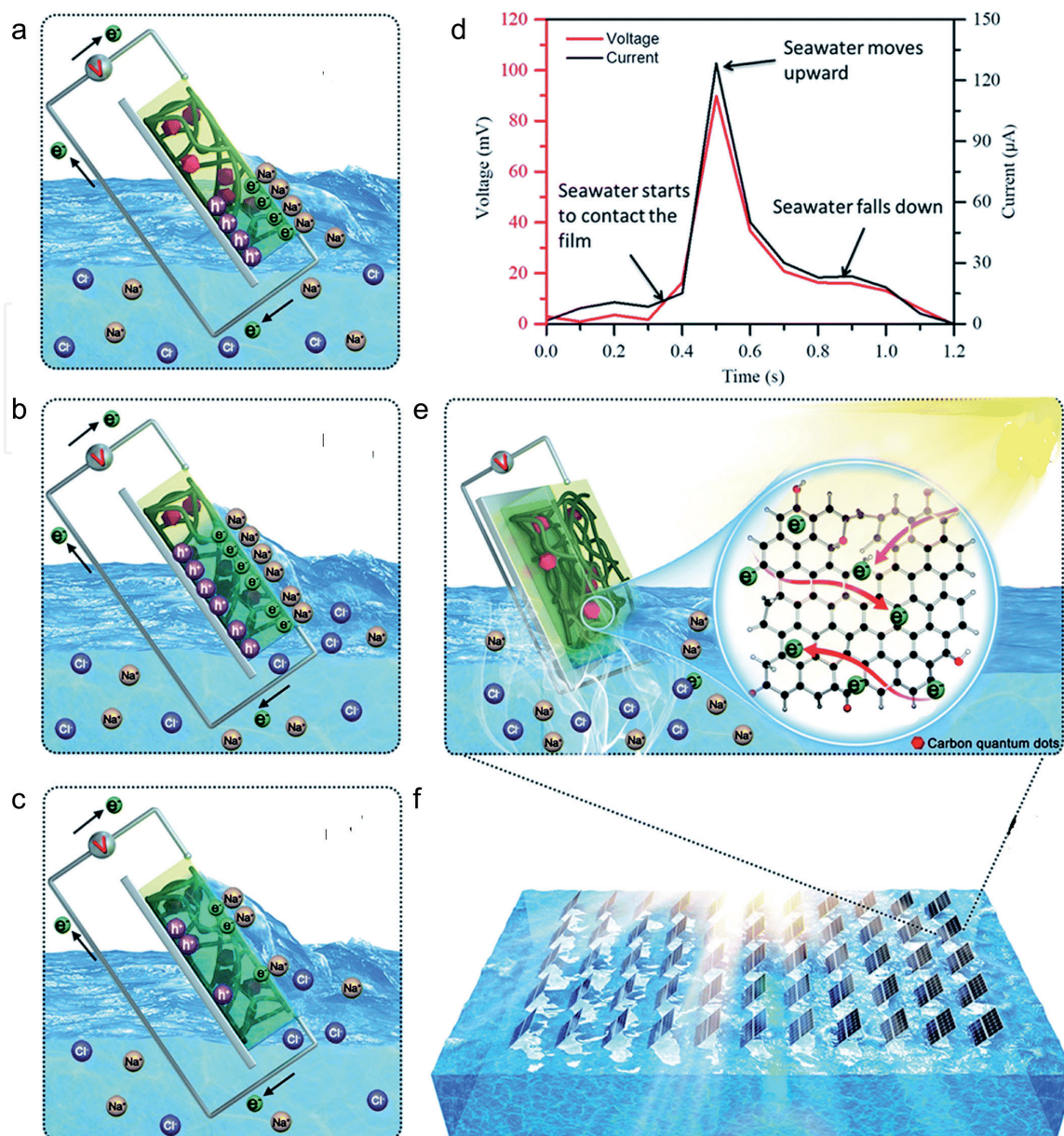


Figure 11.

(a) When the ocean wave meets with the PU/GO-CB-MWCNT/CQDs film, an EDL is generated due to the formation of Na⁺ cation layer and electron layer [25]. (b) When the ocean wave reaches the top of the film, a highest voltage can be observed due to the charge of EDL [25]. (c) When the ocean wave is falling downward, a decreasing voltage is obtained because of the discharging of EDL [25]. (d) the voltage and current change of HV cell in one cycle of ocean wave change [25]. (e) under illumination, the electron density is enhanced with CQDs through light excitation [25]. (f) Illustration of the HV networks assembled with HV cells in series and/or parallel. This network can float on the ocean and harvest wave energy and solar energy [25].

highest position, the maximum peak electricity signal is obtained. In this work, CQDs are used for visible light absorption in the range of 330–490 nm. Then more electrons can be excited, the surface electron density increased as in **Figure 11e**. The authors lastly proposed a circuit design for scaling up the power output in large-scale networks (**Figure 11f**). However, a cost-effective, stable, and promising scalable approach for efficiently harvesting ocean wave energy is an open question.

5. Challenges and perspectives

As shown in **Table 1**, the performance of reported HV devices based on the carbon materials is summarized. Even though the great progress has been achieved in recent years, there are several challenges to overcome in the future. The challenges

include the following: (i) the power is far from the need of practical applications. (ii) The stability and durability in real environment is not clear. (iii) It is difficult to achieve large-scale integrated applications. (iv) More advanced experimental technologies should be developed to reveal the unclear mechanism. (v) Non-carbon hydrovoltaic materials should be synthesized or constructed.

Nowadays, the research of hydrovoltaic materials and technologies is still in its infancy. To solve the above issues, we may try to follow the following approaches. (i) Understand the interaction mechanism between water and carbon for the further improvement of hydrovoltaic device performance. This requires to controllably modify the electronic structure of carbon and manipulate the molecules/ions in flows. For example, heteroatom doping can be adopted to tune the electric properties. (ii) The composition and nanostructure of carbon materials can significantly affect the capability of electricity generation. Therefore the nanostructure should be optimized to enhance the effective surface area. Moreover, the composition tailoring can enhance the conductivity, reducing the loss during charge transport. (iii) To improve the output of hydrovoltaic devices, the carbon materials can be combined with other functional materials, such as photovoltaic materials, ferroelectric material, and piezoelectric materials. This route can additionally convert the solar energy and mechanical energy for higher voltage and current outputs. (iv) Develop new nanomaterials with hydrovoltaic properties. For example, graphdiyne as a new 2D carbon material has unique sp and sp^2 hybridized electronic structure, high theoretical conductivity, good chemical activity, good physical stability, and the intrinsic bandgap of ~ 0.5 eV. Moreover, the synthesis temperature is usually below 100°C . We believe this new carbon material will exhibit unique hydrovoltaic properties. (v) Some in situ and in operando technologies should be used to characterize the interface between water and solid at atom/nano level, such as atomic force microscopy, infrared/Raman spectroscopy, AC impedance spectroscopy, and so on. Nevertheless, hydrovoltaic materials and technologies are very promising for harvesting energy in water. More research efforts should be devoted to realize the practical applications in the near future. In hydrovoltaic field, China stands in the forefront of the world. To realize the practical applications, the multidisciplinary collaboration in research, the government support, and the market promotion are urgent needed in the following decade years.

6. Conclusions

In summary, we introduced the water-carbon interactions and the popular mechanisms of hydrovoltaic effects and reviewed the recent progress of hydrovoltaic devices. This field is in its infancy but is a promising direction in the future. Great achievements in moisture, droplet, flow, and evaporation-induced electricity generation have been gained. Since water evaporation is uninterrupted and available under any conditions, the hydrovoltaic devices have great advantages over other energy conversion devices if the power could meet the daily usage. As in **Table 1**, it is exciting that the optimized hydrovoltaic devices now can generate voltage of 3 V. We believe that the rapid growth will bring this emerging hydrovoltaic device into a viable and broad industry technology.

In China, the water resource is around 6% of the Earth's water resource. However, 80% of the water resource is distributed in the South of China. Therefore the energy harvested from water through hydrovoltaic effect, not the conventional hydropower station, is an attracting and alternative approach in China because the hydrovoltaic effect can generate electricity from not only the water flow, but also the water moisture, droplet, and evaporation. This future technology is a very

Materials	Substrate	Solution	Flow type	Potential (mV)	Current (μ A)	Refs.
GO film	/	DI water	Moisture	700	25	[42]
GO framework	/	DI water	Moisture	260	/	[16]
GO film	/	DI water	Moisture	1500	136	[43]
GO film	/	DI water	Moisture	700	0.2	[44]
GO	/	DI water	Moisture	340	~1	[45]
GO nanoribbon	/	DI water	Moisture	40	300	[46]
GQDs	PET	DI water	Moisture	270	/	[14]
Wrinkled graphene	SiO ₂ /Si	NaCl	Moisture	20	0.045	[17]
Monolayer reduced GO	ITO/PET	Simulated raindrops	Droplet	0.1	0.49	[38]
Graphene/carbon black/PTFE	ITO/FTO	Simulated raindrops	Droplet	0.228	5.97	[18]
Monolayer graphene	SiO ₂ /Si	DI water	Droplet	28.14	1800	[39]
Monolayer graphene	PVDF	DI water	Droplet	100	/	[47]
Monolayer graphene	SiO ₂ /Si	DI water	Droplet	10	0.5	[48]
Nitrogen-doped graphene	SiO ₂ /Si	DI water	Droplet	380	/	[49]
Graphene grid	PDMS	NaCl	Droplet	0.1	/	[50]
Monolayer graphene	SiO ₂ /Si	NaCl	Droplet	0.15	/	[11]
Monolayer graphene	PET etc.	NaCl	Droplet	500	/	[51]
Graphene foam	/	DI water	Flow	0.001	100	[52]
Reduced GO	Paper-pencil	DI water/MgCl ₂	Flow	280	812.5	[53]
Graphene/carbon black	Glass, etc.	Simulated waving	Flow	11.14	3	[25]
Monolayer graphene	PET	NaCl	Flow	100	11	[10]
Carbon black	Quartz	DI water	Flow	1000	0.15	[29]
Graphene hydrogel membrane	/	NaCl	Flow	/	0.002	[54]
Few-layer graphene	SiO ₂ /Si	HCl	Flow	25	340	[55]
Few-layer graphene	SiO ₂ /Si	HCl	Flow	120	/	[56]
Pair of graphene sheets	/	NaCl	Flow	1000	2	[24]
Aligned CNT fiber	/	NaCl	Flow	341	/	[22]
Carbon black film		DI water	Evaporation	1000	/	[29]
Carbon Film	Al ₂ O ₃	DI water	Evaporation	1000	0.6	[57]
Graphene/carbon cloth	/	NaCl	Evaporation	370	/	[58]
Carbon black-glass fiber hybrid film	/	DI water	Evaporation	3000	/	[30]
Partially reduced GO sponge	/	DI water	Evaporation	630	~100	[59]

PMMA, polymethyl methacrylate; PVDF, polyvinylidene fluoride; ITO, indium tin oxide; FTO, fluorine-doped tin oxide; PDMS, polydimethylsiloxane.

Table 1. Performance summary of reported hydrovoltaic devices based on the carbon materials.

promising solution in the North of China. More importantly, this future technology can harvest ocean wave energy for island power supply in Chinese waters.

Acknowledgements

The authors are grateful for the financial support from the National Natural Science Foundation of China (Grant 21703150), the China Postdoctoral Science Foundation (Grant 2015 M582495), and the Sichuan Science and Technology Program (Grant 2018JY0015).

Conflict of interest

The authors declare no conflict of interest.

Author details

Jiale Xie*, Liuliu Wang, Xiaoying Chen, Pingping Yang, Fengkai Wu
and Yuelong Huang
Institute of Photovoltaics, Southwest Petroleum University, Chengdu,
People's Republic of China

*Address all correspondence to: jialexie@swpu.edu.cn

IntechOpen

© 2019 The Author(s). Licensee IntechOpen. This chapter is distributed under the terms of the Creative Commons Attribution License (<http://creativecommons.org/licenses/by/3.0>), which permits unrestricted use, distribution, and reproduction in any medium, provided the original work is properly cited. 

References

- [1] Zhang Z et al. Emerging hydrovoltaic technology. *Nature Nanotechnology*. 2018;**13**(12):1109-1119. DOI: 10.1038/s41565-018-0228-6
- [2] Roger I, Shipman MA, Symes MD. Earth-abundant catalysts for electrochemical and photoelectrochemical water splitting. *Nature Reviews Chemistry*. 2017;**1**(1):0003. DOI: 10.1038/s41570-016-0003
- [3] Salamanca JM, Alvarez-Silva O, Tadeo F. Potential and analysis of an osmotic power plant in the Magdalena River using experimental field-data. *Energy*. 2019;**180**:548-555. DOI: 10.1016/j.energy.2019.05.048
- [4] Husain AAF et al. A review of transparent solar photovoltaic technologies. *Renewable and Sustainable Energy Reviews*. 2018;**94**:779-791. DOI: 10.1016/j.rser.2018.06.031
- [5] Han Y, Zhang Z, Qu L. Power generation from graphene-water interactions. *FlatChem*. 2019;**14**:100090. DOI: 10.1016/j.flatc.2019.100090
- [6] Ghosh S, Sood AK, Kumar N. Carbon nanotube flow sensors. *Science*. 2003;**299**(5609):1042-1044. DOI: 10.1126/science.1079080
- [7] Xu Y, Chen P, Peng H. Generating electricity from water through carbon nanomaterials. *Chemistry – A European Journal*. 2018;**24**(24):6287-6294. DOI: 10.1002/chem.201704638
- [8] Tang Q, Yang P. The era of water-enabled electricity generation from graphene. *Journal of Materials Chemistry A*. 2016;**4**(25):9730-9738. DOI: 10.1039/C6TA03107B
- [9] Stone HA, Stroock AD, Ajdari A. Engineering flows in small devices: Microfluidics toward a lab-on-a-Chip. *Annual Review of Fluid Mechanics*. 2004;**36**(1):381-411. DOI: 10.1146/annurev.fluid.36.050802.122124
- [10] Yin J et al. Waving potential in graphene. *Nature Communications*. 2014;**5**(1):3582. DOI: 10.1038/ncomms4582
- [11] Yin J et al. Generating electricity by moving a droplet of ionic liquid along graphene. *Nature Nanotechnology*. 2014;**9**:378. DOI: 10.1038/nnano.2014.56
- [12] Zhao F et al. Direct power generation from a graphene oxide film under moisture. *Advanced Materials*. 2015;**27**(29):4351-4357. DOI: 10.1002/adma.201501867
- [13] Ponomarenko LA et al. Chaotic Dirac Billiard in graphene quantum dots. *Science*. 2008;**320**(5874):356-358. DOI: 10.1126/science.1154663
- [14] Huang Y et al. Highly efficient moisture-triggered nanogenerator based on graphene quantum dots. *ACS Applied Materials & Interfaces*. 2017;**9**(44):38170-38175. DOI: 10.1021/acsami.7b12542
- [15] Liu K et al. Induced potential in porous carbon films through water vapor absorption. *Angewandte Chemie International Edition*. 2016;**55**(28):8003-8007. DOI: 10.1002/anie.201602708
- [16] Zhao F et al. Highly efficient moisture-enabled electricity generation from graphene oxide frameworks. *Energy & Environmental Science*. 2016;**9**(3):912-916. DOI: 10.1039/C5EE03701H
- [17] Zhen Z et al. A non-covalent cation- π interaction-based humidity-driven electric nanogenerator prepared with salt decorated wrinkled graphene.

- Nano Energy. 2019;**62**:189-196. DOI: 10.1016/j.nanoen.2019.05.026
- [18] Tang Q et al. An all-weather solar cell that can harvest energy from sunlight and rain. Nano Energy. 2016;**30**:818-824. DOI: 10.1016/j.nanoen.2016.09.014
- [19] Wang Y et al. Harvest rain energy by polyaniline-graphene composite films. Renewable Energy. 2018;**125**:995-1002. DOI: 10.1016/j.renene.2018.03.034
- [20] Li J et al. Electricity generation from water droplets via capillary infiltrating. Nano Energy. 2018;**48**:211-216. DOI: 10.1016/j.nanoen.2018.02.061
- [21] Tang W, Chen BD, Wang ZL. Recent progress in power generation from water/liquid droplet interaction with solid surfaces. Advanced Functional Materials. 2019;**29**(41):1901069. DOI: 10.1002/adfm.201901069
- [22] Xu Y et al. A one-dimensional fluidic nanogenerator with a high power conversion efficiency. Angewandte Chemie International Edition. 2017;**56**(42):12940-12945. DOI: 10.1002/anie.201706620
- [23] Liu J, Dai L, Baur JW. Multiwalled carbon nanotubes for flow-induced voltage generation. Journal of Applied Physics. 2007;**101**(6):064312. DOI: 10.1063/1.2710776
- [24] Fei W et al. Waving potential at volt level by a pair of graphene sheets. Nano Energy. 2019;**60**:656-660. DOI: 10.1016/j.nanoen.2019.04.020
- [25] Tan J et al. Generators to harvest ocean wave energy through electrokinetic principle. Nano Energy. 2018;**48**:128-133. DOI: 10.1016/j.nanoen.2018.03.032
- [26] He S et al. Chemical-to-electricity carbon: Water device. Advanced Materials. 2018;**30**(18):1707635. DOI: 10.1002/adma.201707635
- [27] Pei J et al. Liquid flow-induced electricity in carbon nanomaterials. Sustainable Energy & Fuels. 2019;**3**(3):599-610. DOI: 10.1039/C8SE00604K
- [28] Tarelho JPG et al. Graphene-based materials and structures for energy harvesting with fluids – A review. Materials Today. 2018;**21**(10):1019-1041. DOI: 10.1016/j.mattod.2018.06.004
- [29] Xue G et al. Water-evaporation-induced electricity with nanostructured carbon materials. Nature Nanotechnology. 2017;**12**:317. DOI: 10.1038/nnano.2016.300
- [30] Li J et al. Surface functional modification boosts the output of an evaporation-driven water flow nanogenerator. Nano Energy. 2019;**58**:797-802. DOI: 10.1016/j.nanoen.2019.02.011
- [31] Xue J et al. Vapor-activated power generation on conductive polymer. Advanced Functional Materials. 2016;**26**(47):8784-8792. DOI: 10.1002/adfm.201604188
- [32] Yavari F et al. Tunable bandgap in graphene by the controlled adsorption of water molecules. Small. 2010;**6**(22):2535-2538. DOI: 10.1002/sml.201001384
- [33] Bi H et al. Ultrahigh humidity sensitivity of graphene oxide. Scientific Reports. 2013;**3**:2714. DOI: 10.1038/srep02714
- [34] Borini S et al. Ultrafast graphene oxide humidity sensors. ACS Nano. 2013;**7**(12):11166-11173. DOI: 10.1021/nl404889b
- [35] Chen X et al. Scaling up nanoscale water-driven energy conversion into evaporation-driven engines and generators. Nature Communications. 2015;**6**(1):7346. DOI: 10.1038/ncomms8346

- [36] Cheng H et al. Graphene fibers with predetermined deformation as moisture-triggered actuators and robots. *Angewandte Chemie International Edition*. 2013;**52**(40):10482-10486. DOI: 10.1002/anie.201304358
- [37] Liu Z et al. Surface-energy generator of single-walled carbon nanotubes and usage in a self-powered system. *Advanced Materials*. 2010;**22**(9):999-1003. DOI: 10.1002/adma.200902153
- [38] Tang Q et al. A solar cell that is triggered by sun and rain. *Angewandte Chemie International Edition*. 2016;**55**(17):5243-5246. DOI: 10.1002/anie.201602114
- [39] Zhong H et al. Graphene based two dimensional hybrid nanogenerator for concurrently harvesting energy from sunlight and water flow. *Carbon*. 2016;**105**:199-204. DOI: 10.1016/j.carbon.2016.04.030
- [40] Wang ZL. Catch wave power in floating nets. *Nature*. 2017;**542**(7640):159-160. DOI: 10.1038/542159a
- [41] Tan J et al. Photo-induced charge boosting of liquid–solid electrokinetic generators for efficient wave energy harvesting. *Journal of Materials Chemistry A*. 2019;**7**(10):5373-5380. DOI: 10.1039/C8TA12037D
- [42] Xu T et al. Electric power generation through the direct interaction of pristine graphene-oxide with water molecules. *Small*. 2018;**14**(14):1704473. DOI: 10.1002/smll.201704473
- [43] Huang Y et al. Interface-mediated hygroelectric generator with an output voltage approaching 1.5 volts. *Nature Communications*. 2018;**9**(1):4166. DOI: 10.1038/s41467-018-06633-z
- [44] Liang Y et al. Electric power generation via asymmetric moisturizing of graphene oxide for flexible, printable and portable electronics. *Energy & Environmental Science*. 2018;**11**(7):1730-1735. DOI: 10.1039/C8EE00671G
- [45] Shao C et al. Wearable fiberform hygroelectric generator. *Nano Energy*. 2018;**53**:698-705. DOI: 10.1016/j.nanoen.2018.09.043
- [46] Zhao F et al. Graphene oxide nanoribbon assembly toward moisture-powered information storage. *Advanced Materials*. 2017;**29**(3):1604972. DOI: 10.1002/adma.201604972
- [47] Zhong H et al. Graphene-piezoelectric material heterostructure for harvesting energy from water flow. *Advanced Functional Materials*. 2017;**27**(5):1604226. DOI: 10.1002/adfm.201604226
- [48] Zhong H et al. Two dimensional graphene nanogenerator by coulomb dragging: Moving van der Waals heterostructure. *Applied Physics Letters*. 2015;**106**(24):243903. DOI: 10.1063/1.4922800
- [49] Okada T et al. Role of doped nitrogen in graphene for flow-induced power generation. *Advanced Engineering Materials*. 2018;**20**(11):1800387. DOI: 10.1002/adem.201800387
- [50] He Y et al. Galvanism of continuous ionic liquid flow over graphene grids. *Applied Physics Letters*. 2015;**107**(8):081605. DOI: 10.1063/1.4929745
- [51] Yang S et al. Mechanism of electric power generation from ionic droplet motion on polymer supported graphene. *Journal of the American Chemical Society*. 2018;**140**(42):13746-13752. DOI: 10.1021/jacs.8b07778
- [52] Huang W et al. Power generation from water flowing through three-dimensional graphene foam. *Nanoscale*. 2014;**6**(8):3921-3924. DOI: 10.1039/C3NR04261H

[53] Arun RK et al. Energy generation from water flow over a reduced graphene oxide surface in a paper–pencil device. *Lab on a Chip*. 2016;**16**(18): 3589-3596. DOI: 10.1039/C6LC00820H

[54] Guo W et al. Bio-inspired two-dimensional nanofluidic generators based on a layered graphene hydrogel membrane. *Advanced Materials*. 2013;**25**(42):6064-6068. DOI: 10.1002/adma.201302441

[55] Dhiman P et al. Harvesting energy from water flow over graphene. *Nano Letters*. 2011;**11**(8):3123-3127. DOI: 10.1021/nl2011559

[56] Yin J et al. Harvesting energy from water flow over graphene? *Nano Letters*. 2012;**12**(3):1736-1741. DOI: 10.1021/nl300636g

[57] Ding T et al. All-printed porous carbon film for electricity generation from evaporation-driven water flow. *Advanced Functional Materials*. 2017;**27**(22):1700551. DOI: 10.1002/adfm.201700551

[58] Zhang L, Chen X. Nanofluidics for giant power harvesting. *Angewandte Chemie International Edition*. 2013;**52**(30):7640-7641. DOI: 10.1002/anie.201302707

[59] Zhang G et al. Harvesting environment energy from water-evaporation over free-standing graphene oxide sponges. *Carbon*. 2019;**148**:1-8. DOI: 10.1016/j.carbon.2019.03.041